

1 **Search for a Higgs boson in the diphoton final state using the full**  
2 **CDF data set from  $p\bar{p}$  collisions at  $\sqrt{s} = 1.96$  TeV**

3 T. Aaltonen,<sup>21</sup> B. Álvarez González<sup>z</sup>,<sup>9</sup> S. Amerio,<sup>40</sup> D. Amidei,<sup>32</sup> A. Anastassov<sup>x</sup>,<sup>15</sup>  
4 A. Annovi,<sup>17</sup> J. Antos,<sup>12</sup> G. Apollinari,<sup>15</sup> J.A. Appel,<sup>15</sup> T. Arisawa,<sup>54</sup> A. Artikov,<sup>13</sup>  
5 J. Asaadi,<sup>49</sup> W. Ashmanskas,<sup>15</sup> B. Auerbach,<sup>57</sup> A. Aurisano,<sup>49</sup> F. Azfar,<sup>39</sup> W. Badgett,<sup>15</sup>  
6 T. Bae,<sup>25</sup> A. Barbaro-Galtieri,<sup>26</sup> V.E. Barnes,<sup>44</sup> B.A. Barnett,<sup>23</sup> P. Barria<sup>hh</sup>,<sup>42</sup>  
7 P. Bartos,<sup>12</sup> M. Bauce<sup>ff</sup>,<sup>40</sup> F. Bedeschi,<sup>42</sup> S. Behari,<sup>23</sup> G. Bellettini<sup>gg</sup>,<sup>42</sup> J. Bellinger,<sup>56</sup>  
8 D. Benjamin,<sup>14</sup> A. Beretvas,<sup>15</sup> A. Bhatti,<sup>46</sup> D. Bisello<sup>ff</sup>,<sup>40</sup> I. Bizjak,<sup>28</sup> K.R. Bland,<sup>5</sup>  
9 B. Blumenfeld,<sup>23</sup> A. Bocci,<sup>14</sup> A. Bodek,<sup>45</sup> D. Bortoletto,<sup>44</sup> J. Boudreau,<sup>43</sup> A. Boveia,<sup>11</sup>  
10 L. Brigliadori<sup>ee</sup>,<sup>6</sup> C. Bromberg,<sup>33</sup> E. Brucken,<sup>21</sup> J. Budagov,<sup>13</sup> H.S. Budd,<sup>45</sup> K. Burkett,<sup>15</sup>  
11 G. Busetto<sup>ff</sup>,<sup>40</sup> P. Bussey,<sup>19</sup> A. Buzatu,<sup>31</sup> A. Calamba,<sup>10</sup> C. Calancha,<sup>29</sup> S. Camarda,<sup>4</sup>  
12 M. Campanelli,<sup>28</sup> M. Campbell,<sup>32</sup> F. Canelli,<sup>11,15</sup> B. Carls,<sup>22</sup> D. Carlsmith,<sup>56</sup>  
13 R. Carosi,<sup>42</sup> S. Carrillo<sup>m</sup>,<sup>16</sup> S. Carron,<sup>15</sup> B. Casal<sup>k</sup>,<sup>9</sup> M. Casarsa,<sup>50</sup> A. Castro<sup>ee</sup>,<sup>6</sup>  
14 P. Catastini,<sup>20</sup> D. Cauz,<sup>50</sup> V. Cavaliere,<sup>22</sup> M. Cavalli-Sforza,<sup>4</sup> A. Cerri<sup>f</sup>,<sup>26</sup> L. Cerrito<sup>s</sup>,<sup>28</sup>  
15 Y.C. Chen,<sup>1</sup> M. Chertok,<sup>7</sup> G. Chiarelli,<sup>42</sup> G. Chlachidze,<sup>15</sup> F. Chlebana,<sup>15</sup> K. Cho,<sup>25</sup>  
16 D. Chokheli,<sup>13</sup> W.H. Chung,<sup>56</sup> Y.S. Chung,<sup>45</sup> M.A. Ciocci<sup>hh</sup>,<sup>42</sup> A. Clark,<sup>18</sup> C. Clarke,<sup>55</sup>  
17 G. Compostella<sup>ff</sup>,<sup>40</sup> M.E. Convery,<sup>15</sup> J. Conway,<sup>7</sup> M. Corbo,<sup>15</sup> M. Cordelli,<sup>17</sup> C.A. Cox,<sup>7</sup>  
18 D.J. Cox,<sup>7</sup> F. Crescioli<sup>gg</sup>,<sup>42</sup> J. Cuevas<sup>z</sup>,<sup>9</sup> R. Culbertson,<sup>15</sup> D. Dagenhart,<sup>15</sup> N. d'Ascenzo<sup>w</sup>,<sup>15</sup>  
19 M. Datta,<sup>15</sup> P. de Barbaro,<sup>45</sup> M. Dell'Orso<sup>gg</sup>,<sup>42</sup> L. Demortier,<sup>46</sup> M. Deninno,<sup>6</sup> F. Devoto,<sup>21</sup>  
20 M. d'Errico<sup>ff</sup>,<sup>40</sup> A. Di Canto<sup>gg</sup>,<sup>42</sup> B. Di Ruzza,<sup>15</sup> J.R. Dittmann,<sup>5</sup> M. D'Onofrio,<sup>27</sup>  
21 S. Donati<sup>gg</sup>,<sup>42</sup> P. Dong,<sup>15</sup> M. Dorigo,<sup>50</sup> T. Dorigo,<sup>40</sup> K. Ebina,<sup>54</sup> A. Elagin,<sup>49</sup> A. Eppig,<sup>32</sup>  
22 R. Erbacher,<sup>7</sup> S. Errede,<sup>22</sup> N. Ershaidat<sup>dd</sup>,<sup>15</sup> R. Eusebi,<sup>49</sup> S. Farrington,<sup>39</sup> M. Feindt,<sup>24</sup>  
23 J.P. Fernandez,<sup>29</sup> R. Field,<sup>16</sup> G. Flanagan<sup>u</sup>,<sup>15</sup> R. Forrest,<sup>7</sup> M.J. Frank,<sup>5</sup> M. Franklin,<sup>20</sup>  
24 J.C. Freeman,<sup>15</sup> Y. Funakoshi,<sup>54</sup> I. Furic,<sup>16</sup> M. Gallinaro,<sup>46</sup> J.E. Garcia,<sup>18</sup> A.F. Garfinkel,<sup>44</sup>  
25 P. Garosi<sup>hh</sup>,<sup>42</sup> H. Gerberich,<sup>22</sup> E. Gerchtein,<sup>15</sup> S. Giagu,<sup>47</sup> V. Giakoumopoulou,<sup>3</sup>  
26 P. Giannetti,<sup>42</sup> K. Gibson,<sup>43</sup> C.M. Ginsburg,<sup>15</sup> N. Giokaris,<sup>3</sup> P. Giromini,<sup>17</sup> G. Giurgiu,<sup>23</sup>  
27 V. Glagolev,<sup>13</sup> D. Glenzinski,<sup>15</sup> M. Gold,<sup>35</sup> D. Goldin,<sup>49</sup> N. Goldschmidt,<sup>16</sup> A. Golossanov,<sup>15</sup>  
28 G. Gomez,<sup>9</sup> G. Gomez-Ceballos,<sup>30</sup> M. Goncharov,<sup>30</sup> O. González,<sup>29</sup> I. Gorelov,<sup>35</sup>  
29 A.T. Goshaw,<sup>14</sup> K. Goulios,<sup>46</sup> S. Grinstein,<sup>4</sup> C. Grosso-Pilcher,<sup>11</sup> R.C. Group<sup>53</sup>,<sup>15</sup>  
30 J. Guimaraes da Costa,<sup>20</sup> S.R. Hahn,<sup>15</sup> E. Halkiadakis,<sup>48</sup> A. Hamaguchi,<sup>38</sup> J.Y. Han,<sup>45</sup>

31 F. Happacher,<sup>17</sup> K. Hara,<sup>51</sup> D. Hare,<sup>48</sup> M. Hare,<sup>52</sup> R.F. Harr,<sup>55</sup> K. Hatakeyama,<sup>5</sup>  
 32 C. Hays,<sup>39</sup> M. Heck,<sup>24</sup> J. Heinrich,<sup>41</sup> M. Herndon,<sup>56</sup> S. Hewamanage,<sup>5</sup> A. Hocker,<sup>15</sup>  
 33 W. Hopkins<sup>g</sup>,<sup>15</sup> D. Horn,<sup>24</sup> S. Hou,<sup>1</sup> R.E. Hughes,<sup>36</sup> M. Hurwitz,<sup>11</sup> U. Husemann,<sup>57</sup>  
 34 N. Hussain,<sup>31</sup> M. Hussein,<sup>33</sup> J. Huston,<sup>33</sup> G. Introzzi,<sup>42</sup> M. Iori<sup>jj</sup>,<sup>47</sup> A. Ivanov<sup>p</sup>,<sup>7</sup> E. James,<sup>15</sup>  
 35 D. Jang,<sup>10</sup> B. Jayatilaka,<sup>14</sup> E.J. Jeon,<sup>25</sup> S. Jindariani,<sup>15</sup> M. Jones,<sup>44</sup> K.K. Joo,<sup>25</sup> S.Y. Jun,<sup>10</sup>  
 36 T.R. Junk,<sup>15</sup> T. Kamon<sup>25, 49</sup> P.E. Karchin,<sup>55</sup> A. Kasmi,<sup>5</sup> Y. Kato<sup>o</sup>,<sup>38</sup> W. Ketchum,<sup>11</sup>  
 37 J. Keung,<sup>41</sup> V. Khotilovich,<sup>49</sup> B. Kilminster,<sup>15</sup> D.H. Kim,<sup>25</sup> H.S. Kim,<sup>25</sup> J.E. Kim,<sup>25</sup>  
 38 M.J. Kim,<sup>17</sup> S.B. Kim,<sup>25</sup> S.H. Kim,<sup>51</sup> Y.K. Kim,<sup>11</sup> Y.J. Kim,<sup>25</sup> N. Kimura,<sup>54</sup> M. Kirby,<sup>15</sup>  
 39 S. Klimenko,<sup>16</sup> K. Knoepfel,<sup>15</sup> K. Kondo<sup>a</sup>,<sup>54</sup> D.J. Kong,<sup>25</sup> J. Konigsberg,<sup>16</sup> A.V. Kotwal,<sup>14</sup>  
 40 M. Kreps,<sup>24</sup> J. Kroll,<sup>41</sup> D. Krop,<sup>11</sup> M. Kruse,<sup>14</sup> V. Krutelyov<sup>c</sup>,<sup>49</sup> T. Kuhr,<sup>24</sup> M. Kurata,<sup>51</sup>  
 41 S. Kwang,<sup>11</sup> A.T. Laasanen,<sup>44</sup> S. Lami,<sup>42</sup> S. Lammel,<sup>15</sup> M. Lancaster,<sup>28</sup> R.L. Lander,<sup>7</sup>  
 42 K. Lannon<sup>y</sup>,<sup>36</sup> A. Lath,<sup>48</sup> G. Latino<sup>hh</sup>,<sup>42</sup> T. LeCompte,<sup>2</sup> E. Lee,<sup>49</sup> H.S. Lee<sup>g</sup>,<sup>11</sup> J.S. Lee,<sup>25</sup>  
 43 S.W. Lee<sup>bb</sup>,<sup>49</sup> S. Leo<sup>gg</sup>,<sup>42</sup> S. Leone,<sup>42</sup> J.D. Lewis,<sup>15</sup> A. Limosani<sup>t</sup>,<sup>14</sup> C.-J. Lin,<sup>26</sup>  
 44 M. Lindgren,<sup>15</sup> E. Lipeles,<sup>41</sup> A. Lister,<sup>18</sup> D.O. Litvintsev,<sup>15</sup> C. Liu,<sup>43</sup> H. Liu,<sup>53</sup> Q. Liu,<sup>44</sup>  
 45 T. Liu,<sup>15</sup> S. Lockwitz,<sup>57</sup> A. Loginov,<sup>57</sup> D. Lucchesi<sup>ff</sup>,<sup>40</sup> J. Lueck,<sup>24</sup> P. Lujan,<sup>26</sup> P. Lukens,<sup>15</sup>  
 46 G. Lungu,<sup>46</sup> J. Lys,<sup>26</sup> R. Lysak<sup>e</sup>,<sup>12</sup> R. Madrak,<sup>15</sup> K. Maeshima,<sup>15</sup> P. Maestro<sup>hh</sup>,<sup>42</sup>  
 47 S. Malik,<sup>46</sup> G. Manca<sup>a</sup>,<sup>27</sup> A. Manousakis-Katsikakis,<sup>3</sup> F. Margaroli,<sup>47</sup> C. Marino,<sup>24</sup>  
 48 M. Martínez,<sup>4</sup> P. Mastrandrea,<sup>47</sup> K. Matera,<sup>22</sup> M.E. Mattson,<sup>55</sup> A. Mazzacane,<sup>15</sup>  
 49 P. Mazzanti,<sup>6</sup> K.S. McFarland,<sup>45</sup> P. McIntyre,<sup>49</sup> R. McNulty<sup>j</sup>,<sup>27</sup> A. Mehta,<sup>27</sup> P. Mehtala,<sup>21</sup>  
 50 C. Mesropian,<sup>46</sup> T. Miao,<sup>15</sup> D. Mietlicki,<sup>32</sup> A. Mitra,<sup>1</sup> H. Miyake,<sup>51</sup> S. Moed,<sup>15</sup> N. Moggi,<sup>6</sup>  
 51 M.N. Mondragon<sup>m</sup>,<sup>15</sup> C.S. Moon,<sup>25</sup> R. Moore,<sup>15</sup> M.J. Morello<sup>ii</sup>,<sup>42</sup> J. Morlock,<sup>24</sup>  
 52 P. Movilla Fernandez,<sup>15</sup> A. Mukherjee,<sup>15</sup> Th. Muller,<sup>24</sup> P. Murat,<sup>15</sup> M. Mussini<sup>ee</sup>,<sup>6</sup>  
 53 J. Nachtman<sup>n</sup>,<sup>15</sup> Y. Nagai,<sup>51</sup> J. Naganoma,<sup>54</sup> I. Nakano,<sup>37</sup> A. Napier,<sup>52</sup> J. Nett,<sup>49</sup> C. Neu,<sup>53</sup>  
 54 M.S. Neubauer,<sup>22</sup> J. Nielsen<sup>d</sup>,<sup>26</sup> L. Nodulman,<sup>2</sup> S.Y. Noh,<sup>25</sup> O. Norniella,<sup>22</sup> L. Oakes,<sup>39</sup>  
 55 S.H. Oh,<sup>14</sup> Y.D. Oh,<sup>25</sup> I. Oksuzian,<sup>53</sup> T. Okusawa,<sup>38</sup> R. Orava,<sup>21</sup> L. Ortolan,<sup>4</sup>  
 56 S. Pagan Griso<sup>ff</sup>,<sup>40</sup> C. Pagliarone,<sup>50</sup> E. Palencia<sup>f</sup>,<sup>9</sup> V. Papadimitriou,<sup>15</sup> A.A. Paramonov,<sup>2</sup>  
 57 J. Patrick,<sup>15</sup> G. Pauletta<sup>kk</sup>,<sup>50</sup> M. Paulini,<sup>10</sup> C. Paus,<sup>30</sup> D.E. Pellett,<sup>7</sup> A. Penzo,<sup>50</sup>  
 58 T.J. Phillips,<sup>14</sup> G. Piacentino,<sup>42</sup> E. Pianori,<sup>41</sup> J. Pilot,<sup>36</sup> K. Pitts,<sup>22</sup> C. Plager,<sup>8</sup>  
 59 L. Pondrom,<sup>56</sup> S. Poprocki<sup>g</sup>,<sup>15</sup> K. Potamianos,<sup>44</sup> F. Prokoshin<sup>cc</sup>,<sup>13</sup> A. Pranko,<sup>26</sup>

---

<sup>a</sup> Deceased

60 F. Ptohos<sup>h</sup>,<sup>17</sup> G. Punzi<sup>gg</sup>,<sup>42</sup> A. Rahaman,<sup>43</sup> V. Ramakrishnan,<sup>56</sup> N. Ranjan,<sup>44</sup> I. Redondo,<sup>29</sup>  
61 P. Renton,<sup>39</sup> M. Rescigno,<sup>47</sup> T. Riddick,<sup>28</sup> F. Rimondi<sup>ee</sup>,<sup>6</sup> L. Ristori<sup>42</sup>,<sup>15</sup> A. Robson,<sup>19</sup>  
62 T. Rodrigo,<sup>9</sup> T. Rodriguez,<sup>41</sup> E. Rogers,<sup>22</sup> S. Rolli<sup>i</sup>,<sup>52</sup> R. Roser,<sup>15</sup> F. Ruffini<sup>hh</sup>,<sup>42</sup> A. Ruiz,<sup>9</sup>  
63 J. Russ,<sup>10</sup> V. Rusu,<sup>15</sup> A. Safonov,<sup>49</sup> W.K. Sakumoto,<sup>45</sup> Y. Sakurai,<sup>54</sup> L. Santi<sup>kk</sup>,<sup>50</sup>  
64 K. Sato,<sup>51</sup> V. Saveliev<sup>w</sup>,<sup>15</sup> A. Savoy-Navarro<sup>aa</sup>,<sup>15</sup> P. Schlabach,<sup>15</sup> A. Schmidt,<sup>24</sup>  
65 E.E. Schmidt,<sup>15</sup> T. Schwarz,<sup>15</sup> L. Scodellaro,<sup>9</sup> A. Scribano<sup>hh</sup>,<sup>42</sup> F. Scuri,<sup>42</sup> S. Seidel,<sup>35</sup>  
66 Y. Seiya,<sup>38</sup> A. Semenov,<sup>13</sup> F. Sforza<sup>hh</sup>,<sup>42</sup> S.Z. Shalhout,<sup>7</sup> T. Shears,<sup>27</sup> P.F. Shepard,<sup>43</sup>  
67 M. Shimojima<sup>v</sup>,<sup>51</sup> M. Shochet,<sup>11</sup> I. Shreyber-Tecker,<sup>34</sup> A. Simonenko,<sup>13</sup> P. Sinervo,<sup>31</sup>  
68 K. Sliwa,<sup>52</sup> J.R. Smith,<sup>7</sup> F.D. Snider,<sup>15</sup> A. Soha,<sup>15</sup> V. Sorin,<sup>4</sup> H. Song,<sup>43</sup> P. Squillacioti<sup>hh</sup>,<sup>42</sup>  
69 M. Stancari,<sup>15</sup> R. St. Denis,<sup>19</sup> B. Stelzer,<sup>31</sup> O. Stelzer-Chilton,<sup>31</sup> D. Stentz<sup>x</sup>,<sup>15</sup>  
70 J. Strologas,<sup>35</sup> G.L. Strycker,<sup>32</sup> Y. Sudo,<sup>51</sup> A. Sukhanov,<sup>15</sup> I. Suslov,<sup>13</sup> K. Takemasa,<sup>51</sup>  
71 Y. Takeuchi,<sup>51</sup> J. Tang,<sup>11</sup> M. Tecchio,<sup>32</sup> P.K. Teng,<sup>1</sup> J. Thom<sup>g</sup>,<sup>15</sup> J. Thome,<sup>10</sup>  
72 G.A. Thompson,<sup>22</sup> E. Thomson,<sup>41</sup> D. Toback,<sup>49</sup> S. Tokar,<sup>12</sup> K. Tollefson,<sup>33</sup> T. Tomura,<sup>51</sup>  
73 D. Tonelli,<sup>15</sup> S. Torre,<sup>17</sup> D. Torretta,<sup>15</sup> P. Totaro,<sup>40</sup> M. Trovato<sup>ii</sup>,<sup>42</sup> F. Ukegawa,<sup>51</sup>  
74 S. Uozumi,<sup>25</sup> A. Varganov,<sup>32</sup> F. Vázquez<sup>m</sup>,<sup>16</sup> G. Velez,<sup>15</sup> C. Vellidis,<sup>15</sup> M. Vidal,<sup>44</sup> I. Vila,<sup>9</sup>  
75 R. Vilar,<sup>9</sup> J. Vizán,<sup>9</sup> M. Vogel,<sup>35</sup> G. Volpi,<sup>17</sup> P. Wagner,<sup>41</sup> R.L. Wagner,<sup>15</sup> T. Wakisaka,<sup>38</sup>  
76 R. Wallny,<sup>8</sup> S.M. Wang,<sup>1</sup> A. Warburton,<sup>31</sup> D. Waters,<sup>28</sup> W.C. Wester III,<sup>15</sup> D. Whiteson<sup>b</sup>,<sup>41</sup>  
77 A.B. Wicklund,<sup>2</sup> E. Wicklund,<sup>15</sup> S. Wilbur,<sup>11</sup> F. Wick,<sup>24</sup> H.H. Williams,<sup>41</sup> J.S. Wilson,<sup>36</sup>  
78 P. Wilson,<sup>15</sup> B.L. Winer,<sup>36</sup> P. Wittich<sup>g</sup>,<sup>15</sup> S. Wolbers,<sup>15</sup> H. Wolfe,<sup>36</sup> T. Wright,<sup>32</sup> X. Wu,<sup>18</sup>  
79 Z. Wu,<sup>5</sup> K. Yamamoto,<sup>38</sup> D. Yamato,<sup>38</sup> T. Yang,<sup>15</sup> U.K. Yang<sup>r</sup>,<sup>11</sup> Y.C. Yang,<sup>25</sup>  
80 W.-M. Yao,<sup>26</sup> G.P. Yeh,<sup>15</sup> K. Yi<sup>n</sup>,<sup>15</sup> J. Yoh,<sup>15</sup> K. Yorita,<sup>54</sup> T. Yoshida<sup>l</sup>,<sup>38</sup> G.B. Yu,<sup>14</sup>  
81 I. Yu,<sup>25</sup> S.S. Yu,<sup>15</sup> J.C. Yun,<sup>15</sup> A. Zanetti,<sup>50</sup> Y. Zeng,<sup>14</sup> C. Zhou,<sup>14</sup> and S. Zucchelli<sup>ee6</sup>

82 (CDF Collaboration<sup>b</sup>)

<sup>b</sup> With visitors from <sup>a</sup>Istituto Nazionale di Fisica Nucleare, Sezione di Cagliari, 09042 Monserrato (Cagliari), Italy, <sup>b</sup>University of CA Irvine, Irvine, CA 92697, USA, <sup>c</sup>University of CA Santa Barbara, Santa Barbara, CA 93106, USA, <sup>d</sup>University of CA Santa Cruz, Santa Cruz, CA 95064, USA, <sup>e</sup>Institute of Physics, Academy of Sciences of the Czech Republic, Czech Republic, <sup>f</sup>CERN, CH-1211 Geneva, Switzerland, <sup>g</sup>Cornell University, Ithaca, NY 14853, USA, <sup>h</sup>University of Cyprus, Nicosia CY-1678, Cyprus, <sup>i</sup>Office of Science, U.S. Department of Energy, Washington, DC 20585, USA, <sup>j</sup>University College Dublin, Dublin 4, Ireland, <sup>k</sup>ETH, 8092 Zurich, Switzerland, <sup>l</sup>University of Fukui, Fukui City, Fukui Prefecture, Japan 910-0017, <sup>m</sup>Universidad Iberoamericana, Mexico D.F., Mexico, <sup>n</sup>University of Iowa, Iowa City, IA 52242, USA, <sup>o</sup>Kinki University, Higashi-Osaka City, Japan 577-8502, <sup>p</sup>Kansas State University, Manhattan, KS 66506, USA, <sup>q</sup>Ewha Womans University, Seoul, 120-750, Korea, <sup>r</sup>University of Manchester, Manchester

83  
84  
85  
86  
87  
88  
89  
90  
91  
92  
93  
94  
95  
96  
97  
98  
99  
100  
101  
102  
103  
104  
105  
106  
107  
108  
109  
110  
111

<sup>1</sup>*Institute of Physics, Academia Sinica,  
Taipei, Taiwan 11529, Republic of China*

<sup>2</sup>*Argonne National Laboratory, Argonne, Illinois 60439, USA*

<sup>3</sup>*University of Athens, 157 71 Athens, Greece*

<sup>4</sup>*Institut de Fisica d'Altes Energies, ICREA,  
Universitat Autònoma de Barcelona,  
E-08193, Bellaterra (Barcelona), Spain*

<sup>5</sup>*Baylor University, Waco, Texas 76798, USA*

<sup>6</sup>*Istituto Nazionale di Fisica Nucleare Bologna,  
<sup>ee</sup>University of Bologna, I-40127 Bologna, Italy*

<sup>7</sup>*University of California, Davis, Davis, California 95616, USA*

<sup>8</sup>*University of California, Los Angeles,  
Los Angeles, California 90024, USA*

<sup>9</sup>*Instituto de Fisica de Cantabria, CSIC-University of Cantabria, 39005 Santander, Spain*

<sup>10</sup>*Carnegie Mellon University, Pittsburgh, Pennsylvania 15213, USA*

<sup>11</sup>*Enrico Fermi Institute, University of Chicago, Chicago, Illinois 60637, USA*

<sup>12</sup>*Comenius University, 842 48 Bratislava,  
Slovakia; Institute of Experimental Physics, 040 01 Kosice, Slovakia*

<sup>13</sup>*Joint Institute for Nuclear Research, RU-141980 Dubna, Russia*

<sup>14</sup>*Duke University, Durham, North Carolina 27708, USA*

<sup>15</sup>*Fermi National Accelerator Laboratory, Batavia, Illinois 60510, USA*

<sup>16</sup>*University of Florida, Gainesville, Florida 32611, USA*

<sup>17</sup>*Laboratori Nazionali di Frascati, Istituto Nazionale  
di Fisica Nucleare, I-00044 Frascati, Italy*

<sup>18</sup>*University of Geneva, CH-1211 Geneva 4, Switzerland*

<sup>19</sup>*Glasgow University, Glasgow G12 8QQ, United Kingdom*

<sup>20</sup>*Harvard University, Cambridge, Massachusetts 02138, USA*

<sup>21</sup>*Division of High Energy Physics, Department of Physics,*

*University of Helsinki and Helsinki Institute of Physics, FIN-00014, Helsinki, Finland*

---

Institute of Applied Science, Nagasaki, Japan, <sup>w</sup>National Research Nuclear University, Moscow, Russia, <sup>x</sup>Northwestern University, Evanston, IL 60208, USA, <sup>y</sup>University of Notre Dame, Notre Dame, IN 46556, USA, <sup>z</sup>Universidad de Oviedo, E-33007 Oviedo, Spain, <sup>aa</sup>CNRS-IN2P3, Paris, F-75205 France, <sup>bb</sup>Texas Tech University, Lubbock, TX 79609, USA, <sup>cc</sup>Universidad Tecnica Federico Santa Maria, 110v Valparaiso, Chile, <sup>dd</sup>Yarmouk University, Irbid 211-63, Jordan,

112 <sup>22</sup>*University of Illinois, Urbana, Illinois 61801, USA*

113 <sup>23</sup>*The Johns Hopkins University, Baltimore, Maryland 21218, USA*

114 <sup>24</sup>*Institut für Experimentelle Kernphysik,*

115 *Karlsruhe Institute of Technology, D-76131 Karlsruhe, Germany*

116 <sup>25</sup>*Center for High Energy Physics: Kyungpook National University,*

117 *Daegu 702-701, Korea; Seoul National University, Seoul 151-742,*

118 *Korea; Sungkyunkwan University, Suwon 440-746,*

119 *Korea; Korea Institute of Science and Technology Information,*

120 *Daejeon 305-806, Korea; Chonnam National University, Gwangju 500-757,*

121 *Korea; Chonbuk National University, Jeonju 561-756, Korea*

122 <sup>26</sup>*Ernest Orlando Lawrence Berkeley National Laboratory, Berkeley, California 94720, USA*

123 <sup>27</sup>*University of Liverpool, Liverpool L69 7ZE, United Kingdom*

124 <sup>28</sup>*University College London, London WC1E 6BT, United Kingdom*

125 <sup>29</sup>*Centro de Investigaciones Energeticas*

126 *Medioambientales y Tecnologicas, E-28040 Madrid, Spain*

127 <sup>30</sup>*Massachusetts Institute of Technology,*

128 *Cambridge, Massachusetts 02139, USA*

129 <sup>31</sup>*Institute of Particle Physics: McGill University, Montréal,*

130 *Québec, Canada H3A 2T8; Simon Fraser University, Burnaby,*

131 *British Columbia, Canada V5A 1S6; University of Toronto,*

132 *Toronto, Ontario, Canada M5S 1A7; and TRIUMF,*

133 *Vancouver, British Columbia, Canada V6T 2A3*

134 <sup>32</sup>*University of Michigan, Ann Arbor, Michigan 48109, USA*

135 <sup>33</sup>*Michigan State University, East Lansing, Michigan 48824, USA*

136 <sup>34</sup>*Institution for Theoretical and Experimental Physics, ITEP, Moscow 117259, Russia*

137 <sup>35</sup>*University of New Mexico, Albuquerque, New Mexico 87131, USA*

138 <sup>36</sup>*The Ohio State University, Columbus, Ohio 43210, USA*

139 <sup>37</sup>*Okayama University, Okayama 700-8530, Japan*

140 <sup>38</sup>*Osaka City University, Osaka 588, Japan*

141 <sup>39</sup>*University of Oxford, Oxford OX1 3RH, United Kingdom*

142 <sup>40</sup>*Istituto Nazionale di Fisica Nucleare, Sezione di Padova-Trento,*

143 *<sup>ff</sup>University of Padova, I-35131 Padova, Italy*

144  
145  
146  
147  
148  
149  
150  
151  
152  
153  
154  
155  
156  
157  
158  
159  
160  
161  
162  
163  
164

<sup>41</sup> *University of Pennsylvania, Philadelphia, Pennsylvania 19104, USA*

<sup>42</sup> *Istituto Nazionale di Fisica Nucleare Pisa, <sup>99</sup> University of Pisa,*

<sup>hh</sup> *University of Siena and <sup>ii</sup> Scuola Normale Superiore, I-56127 Pisa, Italy*

<sup>43</sup> *University of Pittsburgh, Pittsburgh, Pennsylvania 15260, USA*

<sup>44</sup> *Purdue University, West Lafayette, Indiana 47907, USA*

<sup>45</sup> *University of Rochester, Rochester, New York 14627, USA*

<sup>46</sup> *The Rockefeller University, New York, New York 10065, USA*

<sup>47</sup> *Istituto Nazionale di Fisica Nucleare, Sezione di Roma 1,*

<sup>jj</sup> *Sapienza Università di Roma, I-00185 Roma, Italy*

<sup>48</sup> *Rutgers University, Piscataway, New Jersey 08855, USA*

<sup>49</sup> *Texas A&M University, College Station, Texas 77843, USA*

<sup>50</sup> *Istituto Nazionale di Fisica Nucleare Trieste/Udine,*

*I-34100 Trieste, <sup>kk</sup> University of Udine, I-33100 Udine, Italy*

<sup>51</sup> *University of Tsukuba, Tsukuba, Ibaraki 305, Japan*

<sup>52</sup> *Tufts University, Medford, Massachusetts 02155, USA*

<sup>53</sup> *University of Virginia, Charlottesville, Virginia 22906, USA*

<sup>54</sup> *Waseda University, Tokyo 169, Japan*

<sup>55</sup> *Wayne State University, Detroit, Michigan 48201, USA*

<sup>56</sup> *University of Wisconsin, Madison, Wisconsin 53706, USA*

<sup>57</sup> *Yale University, New Haven, Connecticut 06520, USA*

(Dated: July 25, 2012)

## Abstract

165 A search for a narrow Higgs boson resonance in the diphoton mass spectrum is presented based  
166 on data corresponding to  $10 \text{ fb}^{-1}$  of integrated luminosity from proton-antiproton collisions at  
167  $\sqrt{s} = 1.96 \text{ TeV}$  collected by the CDF experiment. In addition to searching for a resonance in  
168 the diphoton mass spectrum, we employ a multivariate discriminant technique for the first time  
169 in this channel at CDF. No evidence of signal is observed, and upper limits are set on the cross  
170 section times branching ratio of the resonant state as a function of Higgs boson mass. The limits  
171 are interpreted in the context of the standard model with an expected (observed) limit on the  
172 cross section times branching ratio of 9.9 (17.0) times the standard model prediction at the 95%  
173 credibility level for a Higgs boson mass of  $125 \text{ GeV}/c^2$ . Moreover, a Higgs boson with suppressed  
174 couplings to fermions is excluded for masses below  $114 \text{ GeV}/c^2$  at the 95% credibility level.

175 PACS numbers: 14.80.Bn, 12.38.Qk, 13.85.Rm, 14.80.Ec

## 176 I. INTRODUCTION

177 The standard model (SM) of particle physics has proven to be a robust theory that  
178 accurately describes the properties of elementary particles and the forces of interaction  
179 between them. However, the origin of mass has remained an unsolved mystery for decades.  
180 The SM suggests that particles acquire mass due to interactions with the Higgs field via  
181 spontaneous symmetry breaking [1]. Direct searches at the Large Electron-Positron Collider  
182 (LEP) [2], combined with recent search results from the Tevatron [3] and the Large Hadron  
183 Collider (LHC) [4, 5], exclude all potential SM Higgs boson masses outside the ranges 116.6–  
184 119.4 GeV/ $c^2$  and 122.1–127 GeV/ $c^2$ .

185 In the SM, the branching ratio for a Higgs boson decaying into a photon pair  $\mathcal{B}(H \rightarrow \gamma\gamma)$   
186 is maximal for Higgs boson masses between about 110 and 140 GeV/ $c^2$ . This is a mass range  
187 that is most useful for Higgs boson searches at the Fermilab Tevatron [3] and is favored by  
188 indirect constraints from electroweak observables [6]. The SM  $H \rightarrow \gamma\gamma$  branching ratio  
189 peaks at a value of about 0.23% for a Higgs boson mass  $m_H = 125$  GeV/ $c^2$  [7]. This is  
190 a very small branching ratio; however, the distinctive signal that photons produce in the  
191 detector makes  $H \rightarrow \gamma\gamma$  an appealing search mode. Compared to the dominant decay modes  
192 involving  $b$  quarks, a larger fraction of  $H \rightarrow \gamma\gamma$  events can be identified and the diphoton  
193 invariant mass of these events would cluster in a narrower range, thus providing a better  
194 discriminator against the smoothly distributed background. There are also theories beyond  
195 the standard model that predict a suppressed coupling of a Higgs boson to fermions. In  
196 these “fermiophobic” Higgs boson models, the diphoton decay can be greatly enhanced [8].

197 The Collider Detector at Fermilab (CDF) and D0 experiments at the Tevatron have  
198 searched for both a SM Higgs boson,  $H$ , and a fermiophobic Higgs boson,  $h_f$ , decaying to  
199 two photons [9–12]. The CDF and D0 experiments recently set 95% credibility level (C.L.)  
200 upper limits on the cross section times branching ratio  $\sigma \times \mathcal{B}(H \rightarrow \gamma\gamma)$  relative to the SM  
201 prediction and on  $\mathcal{B}(h_f \rightarrow \gamma\gamma)$  using data corresponding to an integrated luminosity  $\mathcal{L}$  of  
202 7.0 fb $^{-1}$  [13] and 8.2 fb $^{-1}$  [14], respectively. The  $h_f$  result sets a lower limit on  $m_{h_f}$  of  
203 114 GeV/ $c^2$  and 112.9 GeV/ $c^2$ , respectively. These results surpassed for the first time the  
204 109.7 GeV/ $c^2$  mass limit obtained from combined searches at the LEP collider at CERN [8].

205 Recently, the ATLAS and CMS experiments at the LHC at CERN have searched for a SM  
206 Higgs boson decaying to two photons using  $\mathcal{L} = 4.9$  fb $^{-1}$  [15] and 4.8 fb $^{-1}$  [16], respectively.

207 In the low mass range, rates corresponding to less than twice the SM cross section are  
208 excluded at 95% C.L. An excess of nearly  $2\sigma$  is present in both the CMS and ATLAS  
209 results, which could be consistent with a SM Higgs boson with a mass near  $125 \text{ GeV}/c^2$ .

210 In this Letter, we present a search for a Higgs boson decaying to two photons using the  
211 final CDF diphoton data set, corresponding to an integrated luminosity of  $10 \text{ fb}^{-1}$ . This  
212 analysis searches the diphoton mass distribution for a narrow resonance that could reveal  
213 the presence of a SM or fermiophobic Higgs boson, updating the previous CDF result [13]  
214 with more than 40% additional integrated luminosity. We furthermore implement a new  
215 multivariate technique for events that contain two central photons, using both diphoton and  
216 jet kinematic variables to improve the sensitivity for identifying a Higgs boson signal from  
217 the diphoton backgrounds.

## 218 II. HIGGS BOSON SIGNAL MODEL

219 For the SM search, we consider the three most likely production mechanisms at the  
220 Tevatron: gluon fusion (GF); associated production (VH), where a Higgs boson is produced  
221 in association with a  $W$  or  $Z$  boson; and vector boson fusion (VBF), where a Higgs boson  
222 is produced alongside two quark jets. As an example, the SM cross sections for  $m_H =$   
223  $125 \text{ GeV}/c^2$  are  $949.3 \text{ fb}$  [17],  $208.0 \text{ fb}$  [18], and  $65.3 \text{ fb}$  [19], respectively. In the fermiophobic  
224 search, we consider a benchmark model in which a Higgs boson does not couple to fermions,  
225 yet retains its SM couplings to bosons [8]. In this model, the GF process is suppressed and  
226 fermiophobic Higgs boson production is dominated by VH and VBF. With  $\mathcal{L} = 10 \text{ fb}^{-1}$ ,  
227 about 28 (43)  $H \rightarrow \gamma\gamma$  ( $h_f \rightarrow \gamma\gamma$ ) events are predicted to be produced for  $m_H = 125 \text{ GeV}/c^2$ .

228 Only about 25% of these events would produce photons that are absorbed in well-  
229 instrumented regions of the CDF detector and pass the full diphoton selection discussed in  
230 Section III [13]. This fraction, along with the predicted distributions of kinematic variables,  
231 is obtained from a simulation of Higgs boson decays into diphotons. For each Higgs boson  
232 mass hypothesis tested in the range  $100\text{--}150 \text{ GeV}/c^2$ , in  $5 \text{ GeV}/c^2$  steps, signal samples are  
233 developed from the PYTHIA 6.2 [20] Monte Carlo (MC) event generator and a parametrized  
234 response of the CDF II detector [21, 22]. All PYTHIA samples were made with CTEQ5L [23]  
235 parton distribution functions, where the PYTHIA underlying event model is tuned to CDF jet  
236 data [24]. Each signal sample is corrected for multiple interactions and differences between

237 the identification of photons in the simulation and the data [13]. The GF signal is further-  
 238 more corrected based on a higher-order theoretical prediction of the transverse momentum  
 239 distribution [25].

### 240 III. DETECTOR AND EVENT SELECTION

241 We use the CDF II detector [26] to identify photon candidate events produced in  $p\bar{p}$   
 242 collisions at  $\sqrt{s} = 1.96$  TeV. The silicon vertex tracker [27] and the central outer tracker [28],  
 243 contained within a 1.4 T axial magnetic field, measure the trajectories of charged particles  
 244 and determine their momenta. Particles that pass through the outer tracker reach the  
 245 electromagnetic (EM) and hadronic calorimeters [29–31], which are divided into two regions:  
 246 central ( $|\eta| < 1.1$ ) and forward or “plug” ( $1.1 < |\eta| < 3.6$ ). The EM calorimeters contain  
 247 fine-grained shower maximum detectors [32], which measure the shower shape and centroid  
 248 position in the plane transverse to the direction of the shower development.

249 The event selection is the same as in the previous  $H \rightarrow \gamma\gamma$  search [13]. Events with two  
 250 photon candidates are selected and the data are divided into four independent categories  
 251 according to the position and type of the photons. In central-central (CC) events, both  
 252 photon candidates are detected within the fiducial region of the central EM calorimeter  
 253 ( $|\eta| < 1.05$ ); in central-plug (CP) events, one photon candidate is detected in this region  
 254 and the other is in the fiducial region of the plug calorimeter ( $1.2 < |\eta| < 2.8$ ); in central-  
 255 central events with a conversion (C’C), both photon candidates are in the central region,  
 256 but one photon converts and is reconstructed from its  $e^+e^-$  decay products; in central-plug  
 257 events with a conversion (C’P), there is one central conversion candidate together with a  
 258 plug photon candidate.

259 In order to improve sensitivity for the fermiophobic Higgs boson search, the event selection  
 260 is extended by taking advantage of the final-state features present in the VH and VBF  
 261 processes. Because the Higgs boson from these processes will be produced in association  
 262 with a  $W$  or  $Z$  boson, or with two jets, the transverse momentum of the diphoton system  $p_T^{\gamma\gamma}$   
 263 is generally higher relative to the diphoton backgrounds. A requirement of  $p_T^{\gamma\gamma} > 75$  GeV/ $c$   
 264 isolates a region of high  $h_f$  sensitivity, retaining roughly 30% of the signal while removing  
 265 99.5% of the background [12]. Two lower- $p_T^{\gamma\gamma}$  regions,  $p_T^{\gamma\gamma} < 35$  GeV/ $c$  and  $35$  GeV/ $c$  <  
 266  $p_T^{\gamma\gamma} < 75$  GeV/ $c$ , are additionally included and provide about 15% more sensitivity to the

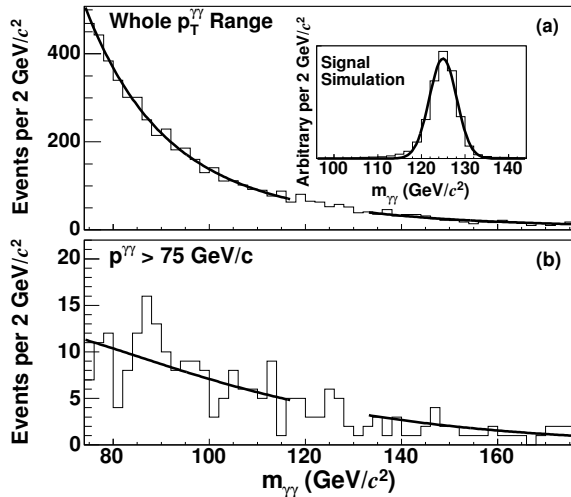


FIG. 1. The invariant mass distribution of CC photon pairs in the data is shown for (a) the entire  $p_T^{\gamma\gamma}$  region used in the SM Higgs boson diphoton resonance search and (b) the highest- $p_T^{\gamma\gamma}$  region (the most sensitive region) used in the  $h_f$  diphoton resonance search. Each distribution shows a fit to the data for the hypothesis of  $m_H = 125 \text{ GeV}/c^2$ , for which the signal region centered at  $125 \text{ GeV}/c^2$  is excluded from the fit. The expected shape of the signal from simulation is shown in the inset of (a).

267  $h_f$  signal. With four diphoton categories (CC, CP, C'C, and C'P) and three  $p_T^{\gamma\gamma}$  regions,  
 268 twelve independent channels are included for the fermiophobic Higgs boson search.

#### 269 IV. DIPHOTON RESONANCE SEARCH

270 The decay of a Higgs boson into a diphoton pair would appear as a very narrow peak in  
 271 the distribution of the invariant mass  $m_{\gamma\gamma}$  of the two photons. The diphoton mass resolution  
 272 as determined from simulation is better than 3% for the Higgs boson mass region studied  
 273 here and is limited by the energy resolution of the electromagnetic calorimeters [33] and  
 274 the ability to identify the primary interaction vertex [13]. The diphoton invariant mass  
 275 distribution for the most sensitive search category in the SM and fermiophobic scenarios is  
 276 provided in Fig. 1, with an inset showing the signal shape expected from simulation. In each  
 277 diphoton category, we perform a search of the  $m_{\gamma\gamma}$  spectrum for signs of a resonance.

278 For this search, the total diphoton background is modeled from a fit to the binned diphoton  
 279 mass spectrum of the data using a log-likelihood ( $\log \mathcal{L}$ ) method, as described in [13].

280 The fit is performed independently for each diphoton category and includes only the sideband  
 281 region for each  $m_H$  hypothesis, which is the control region excluding a mass window centered  
 282 on the Higgs boson mass being tested. The full width of the mass window is chosen to be  
 283 approximately  $\pm 2$  standard deviations of the expected Higgs boson mass resolution, which  
 284 amounts to  $12 \text{ GeV}/c^2$ ,  $16 \text{ GeV}/c^2$ , and  $20 \text{ GeV}/c^2$  for mass hypotheses of  $100\text{--}115 \text{ GeV}/c^2$ ,  
 285  $120\text{--}135 \text{ GeV}/c^2$ , and  $140\text{--}150 \text{ GeV}/c^2$ , respectively. The fit for the CC category for  $m_H =$   
 286  $125 \text{ GeV}/c^2$  is shown in Fig. 1.

## 287 V. MULTIVARIATE DISCRIMINATOR

288 The diphoton mass distribution is the most powerful variable for separating a Higgs  
 289 boson signal from the diphoton backgrounds. However, other information is available that  
 290 can be used to further distinguish this signal. We improve the most sensitive search category  
 291 (CC) by using a “Multi-Layer Perceptron” neural network (NN) [34], which combines the  
 292 information of several well-modeled kinematic variables into a single discriminator, optimized  
 293 to separate signal and background events. Four kinematic variables are included:  $m_{\gamma\gamma}$ ,  $p_T^{\gamma\gamma}$ ,  
 294 the difference between the azimuthal angles of the two photons, and the cosine of the photon  
 295 emission angle relative to the colliding hadrons in the diphoton rest frame (the Collins-Soper  
 296 angle) [35]. For events with jets, we also include four variables related to the jet activity,  
 297 which are particularly useful for identifying VBF and VH signal events. These variables  
 298 are the number of jets in the event, the sum of the jet transverse energies, and the event  
 299 sphericity and aplanarity [36]. Jets are reconstructed from tower clusters in the hadronic  
 300 calorimeter within a cone of radius 0.4 in the  $\eta - \phi$  plane [37]. Each jet is required to have  
 301  $|\eta| < 2$  and a transverse energy  $E_T > 20 \text{ GeV}$ , where the energy is corrected for calorimeter  
 302 response, multiple interactions, and absolute energy scale.

303 In order to optimize the performance of the method, we divide the CC category into two  
 304 independent subsamples of events: the CC0 category for events with no jets and the CCJ  
 305 category for events with at least one jet. The CC0 category uses a network trained with  
 306 only the four diphoton variables; the CCJ category uses a network trained with the four  
 307 diphoton and four jet variables.

308 The sideband fit used in the diphoton resonance search provides an estimate of the to-  
 309 tal background prediction in each signal mass window; however, the multivariate analysis

310 requires a more detailed background model. Specifically, we divide the background into  
 311 its distinct components in order to best model all input variables used by the discriminant,  
 312 which is also sensitive to correlations. There are two main background components in the CC  
 313 data sample: a prompt diphoton ( $\gamma\gamma$ ) background produced from the hard parton scattering  
 314 or from hard photon bremsstrahlung from energetic quarks, and a background comprised  
 315 of  $\gamma$ -jet and jet-jet events ( $\gamma j + jj$ ) in which the jets are misidentified as photons [38]. To  
 316 model the shape of kinematic variables in the  $\gamma\gamma$  background, we use a PYTHIA MC sample  
 317 developed and studied in a measurement of the diphoton cross section [35]. To model the  
 318 variable shapes in the  $\gamma j + jj$  background, we obtain a data sample enriched in misidentified  
 319 photons by selecting events for which one or both photon candidates fail the NN photon ID  
 320 requirement [13].

321 In the diphoton cross section analysis [35] it was found that a  $p_T^{\gamma\gamma}$ -dependent correction  
 322 was needed for the PYTHIA modeling. We adopt the correction for this analysis, reweighting  
 323 the  $p_T^{\gamma\gamma}$  distribution from PYTHIA to match the  $p_T^{\gamma\gamma}$  distribution from control regions in  
 324 prompt diphoton data. For each category, CC0 and CCJ, and for each Higgs boson mass  
 325 hypothesis, event weights are derived based on the sideband regions, excluding the signal  
 326 mass window. The weights are derived by fitting a smooth function to the ratio of the  $p_T^{\gamma\gamma}$   
 327 distribution from the data to that from the PYTHIA prediction. The best fit in the CC0  
 328 category is obtained from a polynomial (constant) function for  $p_T^{\gamma\gamma} < 50 \text{ GeV}/c$  ( $p_T^{\gamma\gamma} >$   
 329  $50 \text{ GeV}/c$ ). A different polynomial (constant) function provides the best fit in the CCJ  
 330 category for  $p_T^{\gamma\gamma} < 60 \text{ GeV}/c$  ( $p_T^{\gamma\gamma} > 60 \text{ GeV}/c$ ). Figure 2 shows the reweighting function  
 331 for a Higgs boson mass hypothesis of  $125 \text{ GeV}/c^2$ . The solid curve shows the best fit to  
 332 the data and the other two curves show the variations induced by propagating the 68%  
 333 C.L. fit uncertainties to the fitting function. The rise of the reweighting function from  
 334  $p_T^{\gamma\gamma} \sim 20 \text{ GeV}/c$  to  $p_T^{\gamma\gamma} \sim 50 \text{ GeV}/c$  in both the CC0 and CCJ categories is interpreted in  
 335 Ref. [35] as an effect of parton fragmentation not modeled in PYTHIA, which contributes to  
 336 the prompt diphoton production cross section in that range.

337 The relative contributions of the two background components are obtained from a fit  
 338 to the diphoton data. Three histograms for each NN input variable are constructed: one  
 339 from the  $\gamma\gamma$  background sample after reweighting, one from the  $\gamma j + jj$  background sample,  
 340 and one from the diphoton data. Events used for the fit are required to have diphoton mass  
 341 values greater than  $70 \text{ GeV}/c^2$  and to be outside of the signal mass window. The histograms

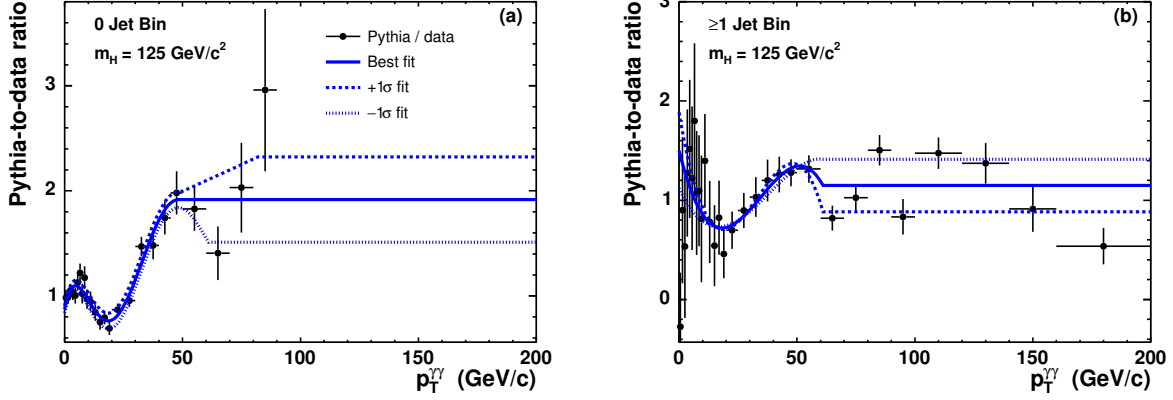


FIG. 2. For a Higgs boson mass of  $125 \text{ GeV}/c^2$ , the reweighting function obtained from the ratio of the  $p_T^{\gamma\gamma}$  distribution in PYTHIA to the  $p_T^{\gamma\gamma}$  distribution in prompt diphoton data, for events with (a) zero jets and (b) at least one jet. In both plots, the best fit to the PYTHIA-to-data ratio points is given by a solid curve. The other two curves show the systematic uncertainty of the fit.

are then used to build a  $\chi^2$  function defined by

$$\chi^2 = \sum_{i=1}^{N_{\text{bins}}} \sum_{j=1}^{N_{\text{variables}}} \left[ \frac{(\alpha g_{ij} + \beta f_{ij} - d_{ij})^2}{d_{ij}} \right] \quad (1)$$

where  $g_{ij}$ ,  $f_{ij}$ , and  $d_{ij}$  refer to the number of events in the  $i$ th bin of the  $j$ th input variable for the prompt  $\gamma\gamma$  background,  $\gamma j + jj$  background, and diphoton data samples, respectively. The sums are over all bins of each input variable for which there are at least 5 events in the data, and the global  $\alpha$  and  $\beta$  coefficients are determined by minimizing the  $\chi^2$  function. This function is defined and minimized separately for each Higgs boson mass hypothesis and for each category (CC0 and CCJ).

A neural network discriminant is trained separately for each mass hypothesis using signal and background events. The signal events used in the training are optimized for the SM scenario and are composed of GF, VH, and VBF PYTHIA samples so that the corresponding total numbers are proportional to their SM cross section predictions. The background sample is made by taking a portion of the  $\gamma j + jj$  sample available for each mass hypothesis and adding  $\gamma\gamma$  events from PYTHIA weighted by the ratio  $\alpha/\beta$  from the  $\chi^2$  fit for the given mass hypothesis.

After training, the NN is applied to the diphoton data sample. Figure 3 shows input variables such as the  $p_T^{\gamma\gamma}$  distribution for events with no reconstructed jets and the sum of the jet  $E_T$  for events with  $\geq 1$  reconstructed jet. The signal shapes are scaled to 20 times the

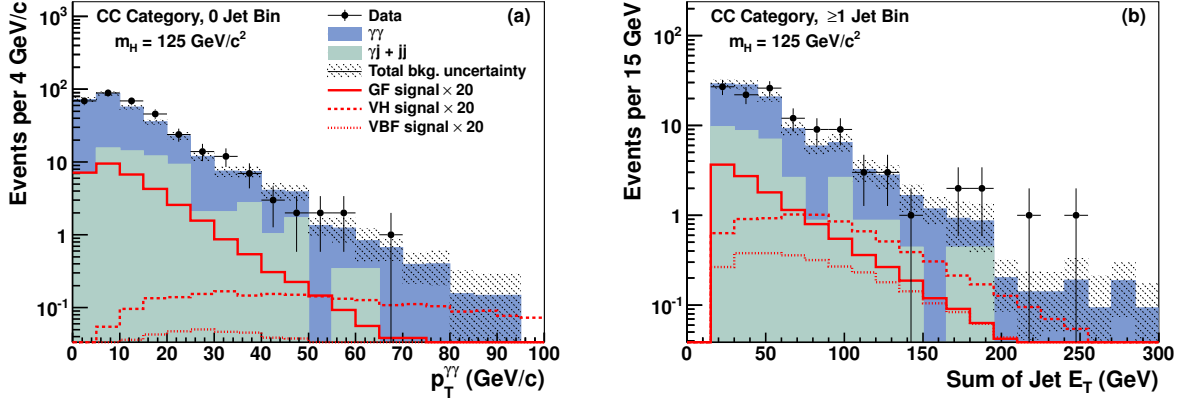


FIG. 3. For a Higgs boson mass of  $125 \text{ GeV}/c^2$ , a comparison of the data to the background prediction in (a) the  $p_T^{\gamma\gamma}$  distribution for the CC0 category and (b) the distribution of the sum of the reconstructed jet  $E_T$  for the CCJ category. The expected Higgs boson signal for the three production processes is multiplied by a factor of 20.

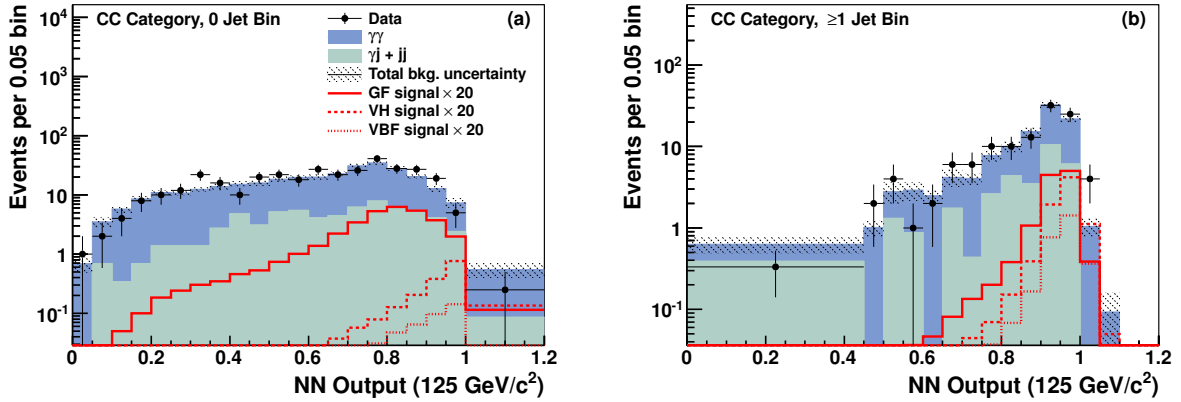


FIG. 4. For a Higgs boson mass of  $125 \text{ GeV}/c^2$ , a comparison of the NN output distributions for the data and the background prediction for (a) the CC0 category and (b) the CCJ category. The expected Higgs boson signal for the three production processes is multiplied by a factor of 20.

359 expected number of reconstructed events in the SM scenario. The background prediction is  
 360 also provided. While the  $\chi^2$  fit described by Eq. (1) is used to fix the relative composition of  
 361 the  $\gamma\gamma$  and  $\gamma j + jj$  background components, the total expected number of background events  
 362 is more accurately determined from sideband mass fits, which is the technique described in  
 363 Section IV. The resulting NN shapes for  $m_H = 125 \text{ GeV}/c^2$  are provided in Figure 4.

## 364 VI. SYSTEMATIC UNCERTAINTIES

365 The sources of systematic uncertainties on the expected number of signal events are  
366 the same as in the previous CDF  $H \rightarrow \gamma\gamma$  search [13]. They arise from the conversion ID  
367 efficiency (7%), the integrated luminosity measurement (6%), varying the parton distribution  
368 functions used in PYTHIA (up to 5%) [39, 40], varying the parameters that control the amount  
369 of initial- and final-state radiation from the parton shower model of PYTHIA (about 4%),  
370 and the PYTHIA modeling of the shape of the  $p_T^{\gamma\gamma}$  distribution for the  $h_f$  signal (up to  
371 4%) [41]. Finally, we include uncertainties from the photon ID efficiency (up to 4%), the  
372 trigger efficiency (less than 3%), and the EM energy scale (less than 1%).

373 The statistical uncertainties on the total background in the signal region are determined  
374 by the fit. They are 3% or less for the channels associated with the SM diphoton resonance  
375 search and are less than 6% for the CC0 and CCJ categories used in the multivariate tech-  
376 nique. For the channels associated with the fermiophobic Higgs boson diphoton resonance  
377 search, the background rate uncertainty is 12% or less, except for the high- $p_T^{\gamma\gamma}$  bins with  
378 conversion photons, where it is 20%.

379 For the search using the multivariate technique, in addition to the rate uncertainties  
380 summarized above, we consider shape uncertainties and bin-by-bin statistical uncertainties  
381 of the NN discriminant. The signal shape uncertainties are associated with initial- and  
382 final-state radiation and the jet energy scale [37], and the background shape uncertainties  
383 are associated with the PYTHIA  $p_T^{\gamma\gamma}$ -correction and the jet energy scale. The PYTHIA shape  
384 uncertainties due to the  $p_T^{\gamma\gamma}$  fits are taken as uncorrelated between the CC0 and the CCJ  
385 categories because the fits determining the corrections for each category are done indepen-  
386 dently. The jet energy scale shape uncertainties are correlated between the two categories in  
387 order to take into account event migration between categories. The dominant uncertainty in  
388 the multivariate analysis is the bin-by-bin statistical uncertainty of the  $\gamma j + jj$  background  
389 histograms.

## 390 VII. RESULTS

391 No evidence of a narrow peak or any other structure is visible in the diphoton mass spec-  
392 trum or the NN output distribution. We calculate a Bayesian C.L. limit for each Higgs boson

393 mass hypothesis based on a combination of likelihoods from the discriminant distributions  
 394 for all channels in the corresponding mass signal region. The combined limits for the SM  
 395 search use the NN discriminants of the CC0 and CCJ categories and the mass discriminants  
 396 from the CP, C'C, and C'P categories. The fermiophobic limits use the NN discriminants  
 397 of the CC0 and CCJ categories and the mass discriminants from the CP, C'C, and C'P  
 398 categories divided into  $p_T^{\gamma\gamma}$  regions. For the limit calculation, we assume a flat prior (trun-  
 399 cated at zero) for the signal rate and a truncated Gaussian prior for each of the systematic  
 400 uncertainties. A 95% C.L. limit is determined such that 95% of the posterior density for  
 401  $\sigma \times \mathcal{B}(H \rightarrow \gamma\gamma)$  falls below the limit [42]. The expected 95% C.L. limits are calculated  
 402 assuming no signal, based on expected backgrounds only, as the median of 2000 simulated  
 403 experiments. The observed 95% C.L. limits on  $\sigma \times \mathcal{B}(H \rightarrow \gamma\gamma)$  are calculated from the  
 404 data.

405 For the SM Higgs boson search, the results are given relative to the theory prediction,  
 406 where theoretical cross section uncertainties of 14% on the GF process, 7% on the VH  
 407 process, and 5% on the VBF process are included in the limit calculation [43]. For the  
 408  $h_f$  model, SM cross sections and uncertainties are assumed (GF excluded) and used to  
 409 convert limits on  $\sigma \times \mathcal{B}(h_f \rightarrow \gamma\gamma)$  into limits on  $\mathcal{B}(h_f \rightarrow \gamma\gamma)$ . The SM and fermiophobic  
 410 limit results for the CC category alone are provided in Table I, showing the gain obtained  
 411 by incorporating a multivariate technique for this category. The combined limit results for  
 412 both searches are displayed in Table II and graphically in Fig. 5. Limits are also provided on  
 413  $\sigma \times \mathcal{B}(H \rightarrow \gamma\gamma)$  for the SM search without including theoretical cross section uncertainties.  
 414 For the SM limit at  $m_H = 120 \text{ GeV}/c^2$ , we observe a deviation of greater than  $2.5\sigma$  from  
 415 the expectation. After accounting for the trials factor associated with performing the search  
 416 at 11 mass points, the significance of this discrepancy decreases to less than  $2\sigma$ . When  
 417 the analysis is optimized for the fermiophobic benchmark model, no excess is observed.  
 418 For the  $h_f$  model, we obtain a limit of  $m_{h_f} < 114 \text{ GeV}/c^2$  by linear interpolation between  
 419 the sampled values of  $m_{h_f}$  based on the intersection of the observed limit and the model  
 420 prediction.

TABLE I. Expected and observed 95% C.L. upper limits on the production cross section multiplied by the  $H \rightarrow \gamma\gamma$  branching ratio relative to the SM prediction for the most sensitive category (CC) using the NN discriminant. For comparison, values for the CC category are also provided based on the diphoton resonance technique, which uses the  $m_{\gamma\gamma}$  shape as a discriminant for setting limits. The expected and observed 95% C.L. upper limits on the  $h_f$  branching ratio (in %) are provided in parentheses, based on both the NN discriminant and diphoton resonance technique for the CC category.

$m_H$ (GeV/ $c^2$ )	NN discriminant		$m_{\gamma\gamma}$ discriminant	
	Expected	Observed	Expected	Observed
100	13.9 (4.6)	10.6 (4.7)	15.1 (5.1)	11.3 (3.5)
105	12.6 (4.6)	13.0 (6.1)	14.1 (5.5)	10.6 (5.1)
110	11.9 (5.2)	11.8 (5.5)	13.5 (5.8)	11.4 (6.3)
115	11.4 (5.2)	14.1 (6.7)	12.9 (6.2)	15.4 (6.0)
120	11.3 (5.5)	23.2 (9.2)	12.8 (6.6)	22.2 (7.3)
125	11.7 (6.4)	20.5 (10.2)	12.9 (6.9)	21.2 (8.0)
130	12.5 (7.0)	13.1 (6.5)	13.9 (7.3)	16.0 (6.0)
135	13.7 (7.7)	15.0 (6.0)	15.3 (7.9)	17.2 (4.9)
140	16.5 (8.2)	20.4 (8.1)	17.5 (8.3)	25.4 (5.9)
145	18.5 (8.4)	27.4 (11.8)	21.2 (8.6)	24.3 (8.8)
150	25.7 (8.7)	17.1 (7.0)	28.2 (9.0)	15.1 (8.4)

## 421 VIII. SUMMARY AND CONCLUSIONS

422 This Letter presents the results of a search for a narrow resonance in the diphoton mass  
423 spectrum using data taken by the CDF II detector at the Tevatron. We have improved  
424 upon the previous CDF analysis by implementing a neural network discriminant to increase  
425 sensitivity in the most sensitive diphoton category by as much as 13%. In addition, we have  
426 included the full CDF data set, which adds more than 40% additional integrated luminosity  
427 relative to the previous diphoton Higgs boson search. There is no significant evidence of a  
428 resonance in the data. Limits are placed on the production cross section times branching

429 ratio for Higgs boson decay into a photon pair and compared to the predictions of the  
 430 standard model and a benchmark fermiophobic model. The latter results in a limit on the  
 431 fermiophobic Higgs boson mass of  $m_{h_f} < 114 \text{ GeV}/c^2$  at the 95% C.L.

TABLE II. Expected and observed 95% C.L. upper limits on the production cross section times branching ratio relative to the SM prediction, the production cross section times branching ratio with theoretical cross section uncertainties removed, and the  $h_f$  branching ratio. The fermiophobic benchmark model prediction for  $\mathcal{B}(h_f \rightarrow \gamma\gamma)$  is also shown for comparison.

	$m_H \text{ (GeV}/c^2)$	100	105	110	115	120	125	130	135	140	145	150
$\sigma \times \mathcal{B}(H \rightarrow \gamma\gamma)/\text{SM}$	Expected	12.2	10.9	10.6	9.7	9.7	9.9	10.5	11.6	14.0	16.0	21.3
	Observed	10.4	11.0	7.7	10.9	21.3	17.0	12.9	12.9	18.3	21.2	14.9
$\sigma \times \mathcal{B}(H \rightarrow \gamma\gamma) \text{ (fb)}$	Expected	45.1	39.0	37.2	31.8	29.7	27.2	25.5	24.0	23.0	20.4	20.2
	Observed	37.9	40.6	26.8	35.9	66.6	47.7	31.5	26.5	30.7	27.2	13.9
$\mathcal{B}(h_f \rightarrow \gamma\gamma) \text{ (%)}$	Expected	3.7	3.8	4.3	4.3	4.6	5.3	5.7	6.1	6.6	6.7	7.1
	Observed	4.9	5.1	3.5	4.8	5.9	4.9	5.3	7.9	8.4	8.3	5.0
	Fermiophobic prediction	18.5	10.4	6.0	3.7	2.3	1.6	1.1	0.8	0.5	0.4	0.3

## 432 ACKNOWLEDGMENTS

433 We thank the Fermilab staff and the technical staffs of the participating institutions for  
 434 their vital contributions. This work was supported by the U.S. Department of Energy and  
 435 National Science Foundation; the Italian Istituto Nazionale di Fisica Nucleare; the Ministry  
 436 of Education, Culture, Sports, Science and Technology of Japan; the Natural Sciences and  
 437 Engineering Research Council of Canada; the National Science Council of the Republic of  
 438 China; the Swiss National Science Foundation; the A.P. Sloan Foundation; the Bundesmin-  
 439 isterium für Bildung und Forschung, Germany; the Korean World Class University Program,  
 440 the National Research Foundation of Korea; the Science and Technology Facilities Coun-  
 441 cil and the Royal Society, UK; the Russian Foundation for Basic Research; the Ministerio  
 442 de Ciencia e Innovación, and Programa Consolider-Ingenio 2010, Spain; the Slovak R&D

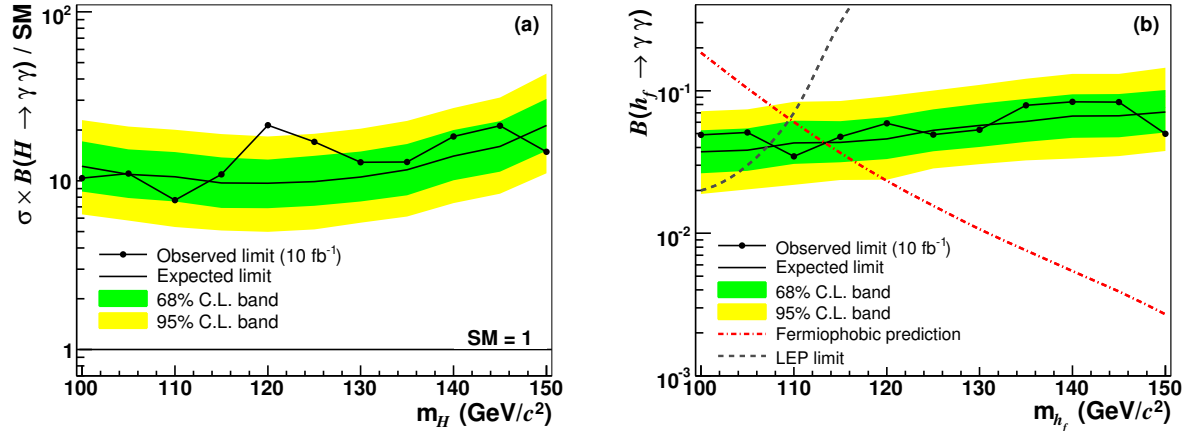


FIG. 5. (a) As a function of  $m_H$ , the 95% C.L. upper limit on the cross section times branching ratio for the SM Higgs boson decay to two photons, relative to the SM prediction. (b) The 95% C.L. upper limit on the branching ratio for the fermiophobic Higgs boson decay to two photons as a function of  $m_{h_f}$ . For reference, the 95% C.L. limits from LEP are also included. The shaded regions represent the 68% C.L. and 95% C.L. bands for the observed limit with respect to the expected limit based on the distribution of simulated experimental outcomes.

443 Agency; the Academy of Finland; and the Australian Research Council (ARC).

- 
- 444 [1] P. W. Higgs, Phys. Rev. Lett. **13**, 508 (1964); G. S. Guralnik, C. R. Hagen, and T. W. B.  
445 Kibble, *ibid.* **13**, 585 (1964); F. Englert and R. Brout, *ibid.* **13**, 321 (1964).  
446 [2] LEP Working Group for Higgs Boson Searches (LEP Collaborations), Phys. Lett. B **565**, 61  
447 (2003).  
448 [3] Tevatron New Phenomena and Higgs Working Group (CDF and D0 Collaborations),  
449 arXiv:1207.0449.  
450 [4] G. Aad *et al.* (ATLAS Collaboration), arXiv:1207.0319.  
451 [5] S. Chatrchyan *et al.* (CMS Collaboration), Phys. Lett. B **710**, 26 (2012).  
452 [6] LEP, Tevatron, and SLD Electroweak Working Groups, arXiv:1012.2367.  
453 [7] A. Djouadi, J. Kalinowski, and M. Spira, Comput. Phys. Commun. **108**, 56 (1998).  
454 [8] A. Rosca (LEP Collaborations), Nucl. Phys. **B**, Proc. Suppl. **117**, 743 (2003); A. G. Akeroyd,  
455 Phys. Lett. B **368**, 89 (1996); A. Barroso, L. Brücher, and R. Santos, Phys. Rev. D **60**,

456 035005 (1999); S. Mrenna and J. Wells, *ibid.* **63**, 015006 (2000); H. E. Haber, G. L. Kane,  
 457 and T. Sterling, Nucl. Phys. **B161**, 493 (1979); J. F. Gunion, R. Vega, and J. Wudka,  
 458 Phys. Rev. D **42**, 1673 (1990); V. Barger, N. G. Deshpande, J. L. Hewett, and T. G. Rizzo,  
 459 arXiv:hep-ph/9211234; J.-L. Basdevant, E. L. Berger, D. Dicus, C. Kao, and S. Willenbrock,  
 460 Phys. Lett. B **313**, 402 (1993); A. Stange, W. Marciano, and S. Willenbrock, Phys. Rev.  
 461 D **49**, 1354 (1994); M. A. Díaz and T. J. Weiler, arXiv:hep-ph/9401259; L. Brücher and  
 462 R. Santos, Eur. Phys. J. C **12**, 87 (2000); G. Landsberg and K. T. Matchev, Phys. Rev. D  
 463 **62**, 035004 (2000).

464 [9] T. Affolder *et al.* (CDF Collaboration), Phys. Rev. D **64**, 092002 (2001).

465 [10] B. Abbott *et al.* (D0 Collaboration), Phys. Rev. Lett. **82**, 2244 (1999).

466 [11] V. M. Abazov *et al.* (D0 Collaboration), Phys. Rev. Lett. **101**, 051801 (2008).

467 [12] T. Aaltonen *et al.* (CDF Collaboration), Phys. Rev. Lett. **103**, 061803 (2009).

468 [13] T. Aaltonen *et al.* (CDF Collaboration), Phys. Rev. Lett. **108**, 011801 (2012).

469 [14] V. M. Abazov *et al.* (D0 Collaboration), Phys. Rev. Lett. **107**, 151801 (2011).

470 [15] G. Aad *et al.* (ATLAS Collaboration), arXiv:1205.0701v1.

471 [16] S. Chatrchyan *et al.* (CMS Collaboration), Phys. Lett. B **710**, 403 (2012).

472 [17] C. Anastasiou, R. Boughezal, and F. Petriello, J. High Energy Phys. 04 (2009) 003; D. de Flo-  
 473 rian and M. Grazzini, Phys. Lett. B **674**, 291 (2009).

474 [18] J. Baglio and A. Djouadi, J. High Energy Phys. 10 (2010) 064; O. Brein, A. Djouadi, and  
 475 R. Harlander, Phys. Lett. B **579**, 149 (2004); M. L. Ciccolini, S. Dittmaier, and M. Krämer,  
 476 Phys. Rev. D **68**, 073003 (2003).

477 [19] P. Bolzoni, F. Maltoni, S.-O. Moch, and M. Zaro, Phys. Rev. Lett. **105**, 011801 (2010);  
 478 M. Ciccolini, A. Denner, and S. Dittmaier, *ibid.* **99**, 161803 (2007); Phys. Rev. D **77**, 013002  
 479 (2008).

480 [20] T. Sjöstrand, P. Edén, C. Friberg, L. Lönnblad, G. Miu, S. Mrenna, and E. Norrbin, Comput.  
 481 Phys. Commun. **135**, 238 (2001).

482 [21] R. Brun *et al.*, CERN Report No. CERN-DD-EE-84-01, 1987.

483 [22] G. Grindhammer, M. Rudowicz, and S. Peters, Nucl. Instrum. Methods Phys. Res., Sect. A  
 484 **290**, 469 (1990).

485 [23] H. L. Lai, *et al.* (CTEQ Collaboration), Eur. Phys. J. C **12**, 375 (2000).

486 [24] T. Aaltonen *et al.* (CDF Collaboration), Phys. Rev. D **82**, 034001 (2010).

- 487 [25] G. Bozzi, S. Catani, D. de Florian, and M. Grazzini, Phys. Lett. B **564**, 65 (2003). G. Bozzi,  
488 S. Catani, D. de Florian, and M. Grazzini, Nucl. Phys. **B737**, 73 (2006). D. de Florian, G.  
489 Ferrera, M. Grazzini, and D. Tommasini, J. High Energy Phys. 11 (2011) 064.
- 490 [26] D. Acosta *et al.* (CDF Collaboration), Phys. Rev. D **71**, 032001 (2005).
- 491 [27] A. Sill (CDF Collaboration), Nucl. Instrum. Methods Phys. Res., Sect. A **447**, 1 (2000).
- 492 [28] T. Affolder *et al.*, Nucl. Instrum. Methods Phys. Res., Sect. A **526**, 249 (2004).
- 493 [29] L. Balka *et al.*, Nucl. Instrum. Methods Phys. Res., Sect. A **267**, 272 (1988).
- 494 [30] S. Bertolucci *et al.*, Nucl. Instrum. Methods Phys. Res., Sect. A **267**, 301 (1988).
- 495 [31] M. Albrow *et al.*, Nucl. Instrum. Methods Phys. Res., Sect. A **480**, 524 (2002).
- 496 [32] G. Apollinari, K. Goulianos, P. Melese, and M. Lindgren, Nucl. Instrum. Methods Phys. Res.,  
497 Sect. A **412**, 515 (1998).
- 498 [33] The energy resolution for photons is  $13.5\%/\sqrt{E_T}$  in the central region and  $(16\%/\sqrt{E_T}) \oplus 1\%$   
499 in the plug region.
- 500 [34] A. Hoecker *et al.*, arXiv:physics/0703039.
- 501 [35] T. Aaltonen *et al.* (CDF Collaboration), Phys. Rev. D **84**, 052006 (2011).
- 502 [36] D. Acosta *et al.* (CDF Collaboration), Phys. Rev. D **72**, 052003 (2005).
- 503 [37] A. Bhatti *et al.* (CDF Collaboration), Nucl. Instrum. Methods Phys. Res., Sect. A **566**, 375  
504 (2006).
- 505 [38] Typically, this occurs when a jet fragments into a  $\pi^0$  or  $\eta$  particle that subsequently decays  
506 to multiple photons, which are then reconstructed as a single photon.
- 507 [39] D. Stump *et al.*, J. High Energy Phys. 10 (2003) 046.
- 508 [40] D. Bourilkov, R. C. Group, and M. R. Whalley, arXiv:hep-ph/0605240.
- 509 [41] S. Mrenna and C.-P. Yuan, Phys. Lett. B **416**, 200 (1998).
- 510 [42] J. Beringer *et al.* (Particle Data Group), Phys. Rev. D **86**, 010001 (2012).
- 511 [43] M. Botje *et al.*, arXiv:1101.0538; S. Dittmaier *et al.* (LHC Higgs Cross Section Working  
512 Group), arXiv:1101.0593.